Materials Physics and Mechanics 16 (2013) 92-100 Received: January 19, 2013

SYNTHESIS, GROWTH AND CHARACTERIZATION OF NOVEL SEMIORGANIC NONLINEAR OPTICAL POTASSIUM BORO-OXALATE (KBO) SINGLE CRYSTALS

Deepa Jananakumar[1*], P. Mani[2]

[1]Department of Physics, Velalar College of Engineering and Technology, Erode, 638009, India

[2]Department of Physics, Hindustan University Padur, Chennai, 603103, India

*e-mail: deepaavanthikaa@yahoo.co.in

Abstract. New semiorganic nonlinear optical (NLO) Potassium Boro-oxalate single crystals have been grown by Slow Evaporation technique at ambient temperature. The title compound has been subjected to single-crystal X-ray diffraction analysis to identify the unit cell parameters. Fourier Transform Infrared spectroscopic analysis was carried out on the grown sample to ascertain the fundamental functional groups. Optical absorption studies illustrate low absorption in the entire UV and Visible region. The crystal was subjected to TGA DTA analysis to find its thermal stability. The dielectric response of the crystal with varying frequencies was studied. The mechanical property of the grown crystals had been analyzed by Vickers's microhardness method. The NLO property of the grown crystal has been confirmed by the Kurtz powder Second Harmonic Generation (SHG) test.

1. Introduction

Nonlinear optics (NLO) is at the vanguard of current research, because of its importance in providing the key functions of frequency shifting, optical modulation, optical switching, optical logic, and optical memory for the emerging techniques in areas such as telecommunications, signal processing and optical interconnections [1, 2]. The NLO phenomena occur when the optical properties of molecules change in the presence of strong external electric fields, i.e., high-energy laser beams. Most organic NLO crystals have usually poor mechanical and thermal properties and are susceptible for damage during processing even though they have large NLO efficiency. Also it is difficult to grow larger size optical-quality crystals of these materials for device applications. Purely inorganic NLO materials have excellent mechanical and thermal properties, but possess relatively modest optical nonlinearity because of the lack of extended π-electron delocalization [3, 4]. Hence it may be useful to prepare semiorganic crystals which combine the positive aspects of organic and inorganic materials, resulting in useful nonlinear optical properties.

The basic requirements for a NLO crystal to be successfully utilized in frequency conversion are a lack of centre of symmetry for the molecular charge transfer, significant change in dipole moment upon excitation from the electronic ground state to some excited states , small to moderate excitation energies of the corresponding excited states , Hammett constants of the substituent, nonzero NLO coefficient, transparency at all wavelengths involved, efficient transfer of energy between the optical waves propagating through the crystal, and good physical (low vapour pressure, high thermostability) and optical (high damage threshold, large birefringence, low dispersion) properties [5, 6].

According to the Philips-Van Vechten-Levine-Xue bond theory [7], constituent chemical bonds of the single crystal determine its NLO responses. Semiorganic materials structurally involve one or more kinds of hydrogen bonds, which have been identified as one of the NLO functional bonds. Semiorganic materials possess several attractive properties such as high damage threshold, wide transparency range, less deliquescence and high non-linear coefficient, which make them suitable for frequency doubling [8, 9].

The extensive search for new types of borate crystals has led to the discovery of many excellent materials such as Lithium bis-L malato borate [10], Potassium boromalate [11], and Potassium borosuccinate [12]. In this sequence, a new semiorganic borate family crystal doped with inorganic salt namely, Potassium Boro-oxalate has been developed.

In the present investigation, we report the bulk growth, crystalline perfection, optical, thermal, dielectric, mechanical, and second harmonic generation (SHG) properties of Potassium Boro-oxalate (KBO) single crystals.

2. Crystal growth

Merck GR grade, Potassium hydroxide, Boric acid and Oxalic acid along with de-ionized water were used for the synthesis and growth. Potassium Boro-oxalate (KBO) was synthesized by equimolar incorporation of Potassium hydroxide, Boric acid and Oxalic acid. The component salt was well dissolved in de-ionized water. Single crystals of KBO were grown by solution growth employing slow evaporation technique at room temperature (31 ^{o}C). For the formation of KBO solution, the amount of solute i.e. (KBO salts) required to prepare the supersaturated solution is given by the formula,

$$m = M \times X \times V/1000 \text{ (in gram units)},$$

where M is the molecular weight of the solute, X is the supersaturated concentration in molar units (1 M in the present work) and V is the required volume of the solution [13].

Fig. 1. As grown single crystals of KBO.

The supersaturated solution was stirred well for 12 hours at room temperature using a temperature controlled magnetic stirrer to yield a homogenous mixture of solution. Then the solution was filtered using a Whatmann filter paper and was transferred in a beaker covered with airtight thick filter paper so that the rate of evaporation can be minimised. Optically

transparent crystals were formed due to spontaneous nucleation. Among them defect free crystals were selected as seeds in order to grow bulk crystals. The synthesized salt was purified by successive recrystallization process. After a period of 30 days single crystals of KBO having dimensions 6x3x2 mm^3 were obtained by isothermal solvent evaporation method at room temperature. The photograph of the as grown crystal is as shown in Fig. 1.

3. Single crystal XRD analysis

The grown crystals were subjected to single crystal x-ray diffraction analysis using an ENRAF NONIUS CAD-4 single crystal X-ray diffractometer with CuK_α radiation (λ=1.5418 Å) to determine the lattice parameters. The calculated lattice parameters are a = 3.74 Å, b = 9.50 Å, c = 17.77 Å, $\alpha = \beta = \gamma = 90^o$. The volume of the unit cell, V = 632 $Å^3$. The crystal belongs to the Orthorhombic system with a noncentrosymmetric space group $P2_12_12_1$.

4. FTIR Analysis

In order to analyze the presence of functional groups qualitatively in the grown crystal, the FTIR spectrum was recorded between 400 cm^{-1} and 4000 cm^{-1} using IFS BRUKER 66V spectrometer by KBr pellet technique and the resultant spectrum is shown in Fig. 2. The broad band at 3056 cm^{-1} is due to O–H stretching. The carbonyl stretching COO^- is found to be near 1700 cm^{-1}. The peak at 1440 cm^{-1} indicates the presence of C–O–H bending. A sharp band observed at 782 cm^{-1} and 924 cm^{-1} has been assigned to the B–O symmetric stretching vibrations. The B–O asymmetric stretching vibrations appear at 1102 cm^{-1}, 1250 cm^{-1} and 1358 cm^{-1} with very strong intensity. The very sharp peak at 1025 cm^{-1} has been attributed to B–O terminal symmetric stretching vibration. A peak at 508 cm^{-1} is assigned to K–O stretching vibration [14, 15]. All these assignments confirm the presence of potassium and borate ions in the crystal lattice of maleic acid and are tabulated in Table 1.

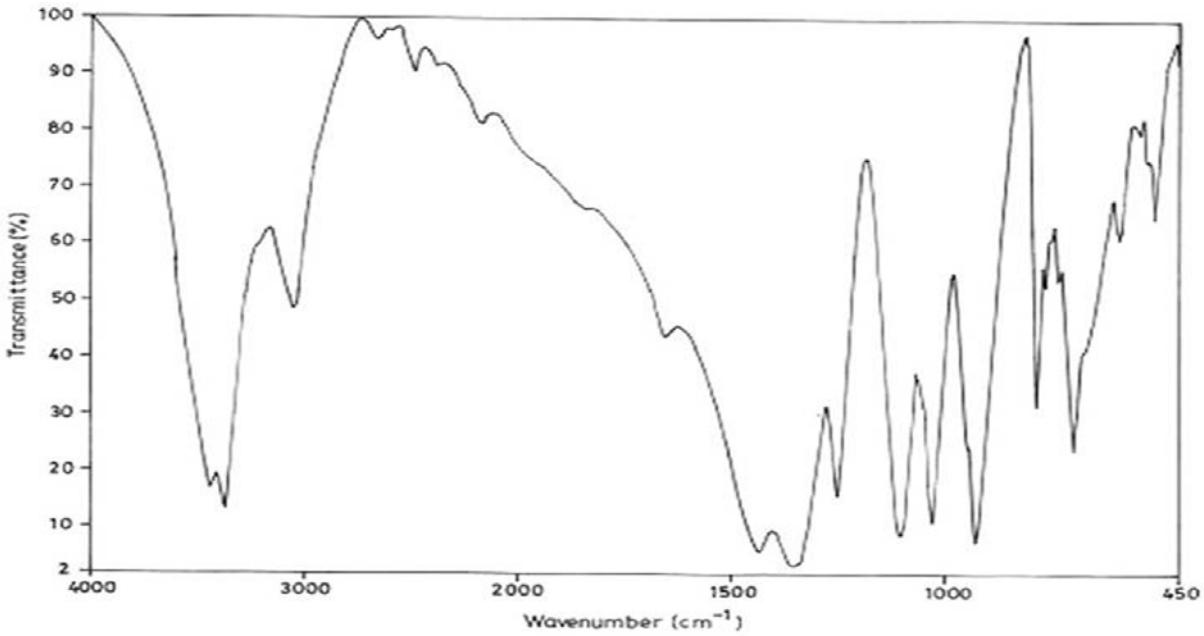

Fig. 2. FTIR spectrum of KBO.

5. UV-VIS-NIR spectral analysis

The absorption spectrum of KBO was recorded in the wavelength range between 190 nm and 1100 nm, using Lamda 35 UV-VIS spectrophotometer (Fig. 3) and its optical transmission

spectrum was recorded in the range 200 nm to 2000 nm using VARIAN CARY 5E spectrophotometer (Fig. 4).

Table 1. Fundamental frequencies of vibrations of KBO crystals.

Frequency wave number, cm^{-1}	Assignment of functional groups
3056	O-H stretching
1700	C=O stretching
1440	C-O-H bending
782	B-O symmetric stretching
924	B-O symmetric stretching
1102	B-O asymmetric stretching
1250	B-O asymmetric stretching
1358	B-O asymmetric stretching
1025	B-O terminal stretching
508	K-O stretching vibrations

The spectrum gives information about the structure of the molecule because the absorption of UV and Visible light involves promotion of the electron in the σ and π orbital from the ground state to higher states [16]. The crystal has excellent transmission in the entire visible region. The lower cut off wavelength is 240 nm. Single crystals are mainly used in optical applications and hence optical transmittance window and the transparency lower cut off (200 nm-400 nm) is very important for the realization of SHG output in this range using lasers. This transparent nature in the visible region is a desirous property for the material used for NLO applications. The forbidden gap energy gap (E_g) of KBO was estimated from the relation $E_g = 1.243\times10^3 / \lambda_{max}$ and is found to be 5.17 eV, which is typical of dielectric materials [17].

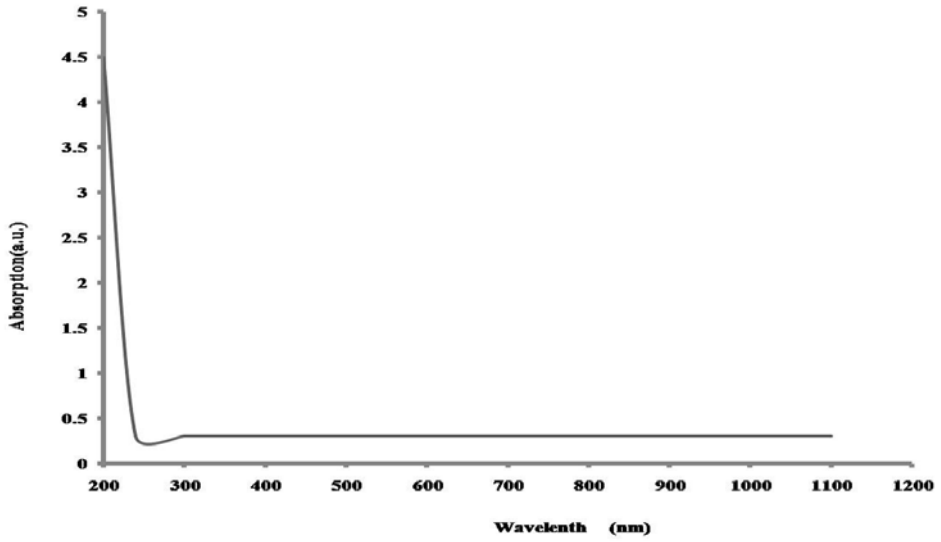

Fig. 3. Absorption spectrum of KBO.

The absence of absorption bands in the visible region and the wide band gap of the grown crystal attest to the suitability of the grown crystal for photonic and optical applications [18]. The larger energy band gap shows that the defect concentration in the grown crystals is very low.

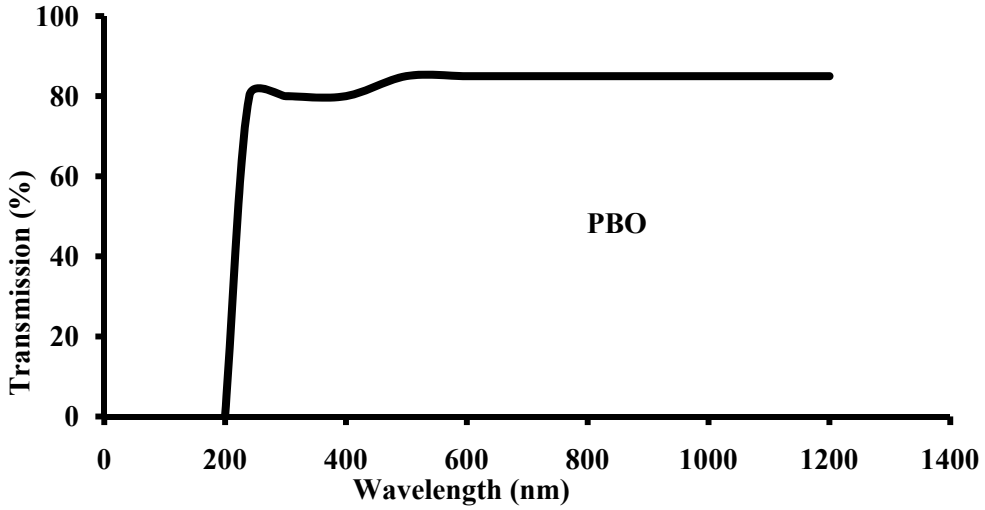

Fig. 4. Transmission spectrum of KBO.

6. Thermal analysis

The thermogravimetric analysis (TG) and differential thermo-gravimetric analysis (DTA) of the KBO crystals were carried out for the sample weight of 22.620 mg between 50 and 1000 °C at a heating rate of 20 K/min in nitrogen atmosphere and the resulting thermogram is shown in the Fig. 5. The TG/DTA curve infers that the melting point of the material takes place in the vicinity of 196 °C. Above 196 °C, the material begins to attain an endothermic transition and starts to decompose at 305.2 °C. The sharpness of this peak shows a good degree of crystallinity and purity of the sample. The DTA thermogram reveals that the material undergoes an irreversible exothermic transition at 210.2 and 784.8 °C. The weight loss at 210.2 and 784.8 °C is due to the liberation of volatile substances like maleate ion, oxides of borons and potassium, leading to significant decomposition of the material. From the thermal study, it can be concluded that the crystal is thermally stable up to 196 °C.

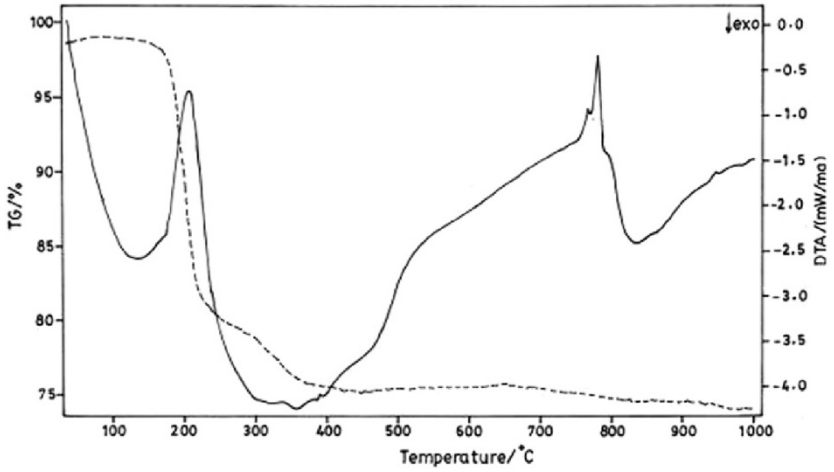

Fig. 5. TGA-DTA analysis.

7. Dielectric characterization

The study of dielectric constant of a material gives an outline about the nature of atoms, ions and their bonding in the material. From the analysis of dielectric constant as a function of frequency and temperature, the different polarization mechanism in solids can be understood. Single crystals of KBO were cut in rectangular dimension of thickness 1 mm and area of cross-section 1 mm^2 is subjected to dielectric studies. The capacitance, the phase angle and the dissipation factor of the parallel plate capacitor formed by copper plate as electrodes and the sample as dielectric medium are measured in the frequency range 1 kHz to 1 MHz The dielectric constant is evaluated using the relation [19]:

$\varepsilon' = Cd/ \varepsilon_0 A,$

where d is the thickness of the sample, A is the area of the sample. The variation of dielectric constant against frequency at room temperature for these crystals is shown in Fig. 6. The profile reveals that the dielectric constant decreases with increase in frequency and it becomes independent of frequency at higher frequency region. The large value dielectric constant at low frequencies can be attributed to the lower electrostatic binding strength, arising due to the space charge polarization near the grain boundary interfaces. The very low value of dielectric constant at higher frequencies are important for these materials in the construction of photonic and NLO devices [20-22].

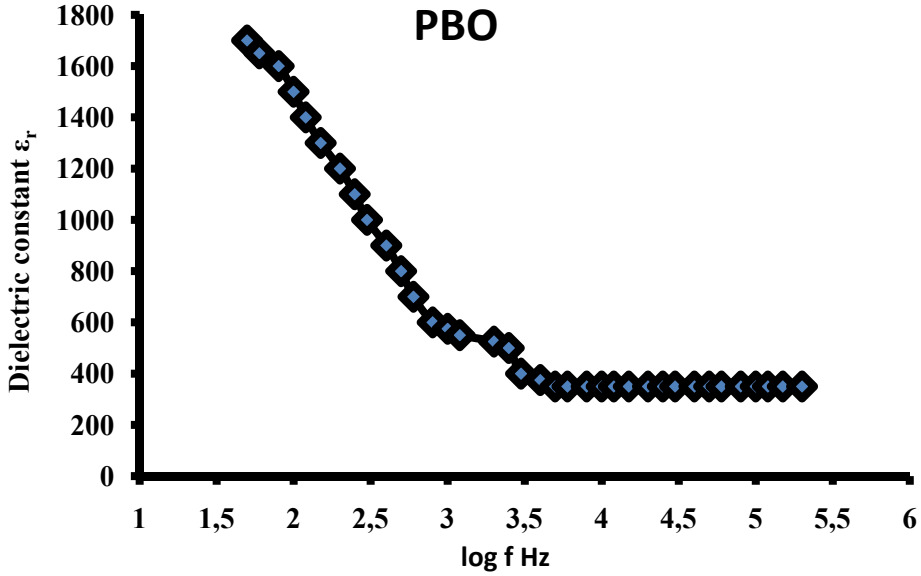

Fig. 6. Variation of dielectric constant vs. log f for KBO.

8. Microhardness study

The microhardness testing is the simplest characterization technique that can be best employed to study the mechanical properties of material, such as fracture behaviour, yield strength, brittleness index and temperature of cracking [21]. The hardness of the material depends on different parameters such as lattice energy, Debye temperature, heat of formation and interatomic spacing [22-24]. According to Ariouli et al. [25], during an indentation process, the external work applied by the indenter is converted to a strain energy component which is proportional to the volume of the resultant impression and the surface energy component is proportional to the area of the resultant impression. Microhardness is a general

microprobe technique to assess the bond strength, apart from being a measure of bulk strength [26-38]. The selected smooth surfaces of the crystal were subjected to indentation tests. For each load several trials of indentations were carried out. The Vickers's microhardness H_v of the crystal was evaluated using the relation $H_v=1.8544\ (P/d^2)$ kg/mm^2 [29], where P is the indenter load in kg and d is the mean diagonal length of the impression in mm. Optically clear and defect free crystal plate taken perpendicular to the growth direction was subjected to indentation tests at room temperature. The diagonal length of the indentation (d) in μ-m for various applied load (P) in g was measured for a constant indentation period of 15 s. Figure 7 shows that the Vickers's hardness number linearly increases by increasing the applied load. Due to the application of mechanical stress by the indenter, dislocations are generated locally in the region of indentation. The Mayer's index number was calculated from the Mayer's law [30], which relates the load and indentation diagonal length:

$P = kd^n, \qquad \log P = \log k + n \log d,$

where k is the material constant and n is the Mayer's index (or work-hardening coefficient). The above relation indicates that H_v should increase with load P if $n>2$ and decrease with load P when $n<2$. We have determined n from slope of the plot that is shown in Fig. 8. The value of n for KBO was found to be 2.7. Low value of work hardening coefficient n illustrates fewer defects [31] in the as grown crystal. According to Onitsch [32], n should lie between 1 and 1.6 for harder materials and above 1.6 for softer materials. By Mayer's law, the value of Mayer's index (n) estimated to be 2.7, which indicates that KBO crystal belongs to soft material category. Meyer number is a measure of the Indentation Size Effect (ISE). For the normal ISE behaviour, the exponent is $n<2$. When $n > 2$, there is the Reverse Indentation Size Effect (RISE) behaviour [33, 34].

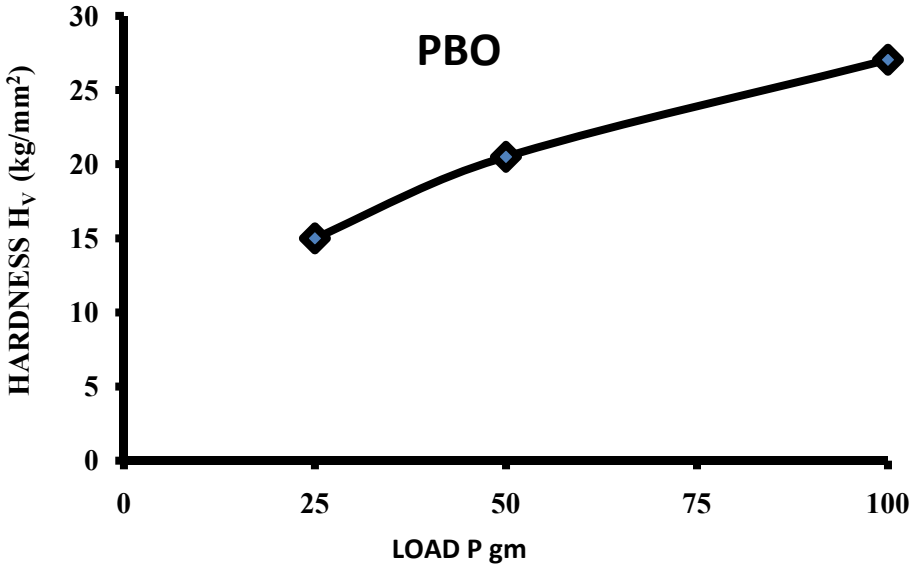

Fig. 7. Hardness of KBO.

9. NLO studies

The nonlinear property in KBO was studied using a Q-switched Nd: YAG laser by employing Kurtz powder test [35, 36]. The fundamental beam of an Nd: YAG laser with 1064 nm wavelength, pulse duration of 35 ns and 10 Hz repetition rate is focused on to the powdered sample. The Second Harmonic Generation (SHG) signal at 532 nm is recorded at various

points on the sample using a photomultiplier tube. The SHG efficiency is found to be 1.5 times greater than that of inorganic sample of Potassium dihydrogen phosphate KDP.

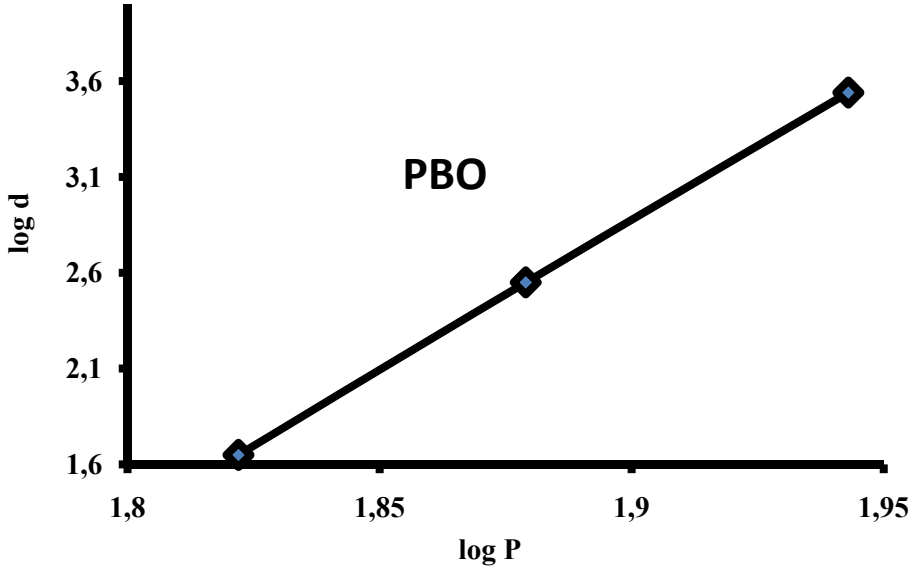

Fig. 8. Plot of log P vs. log d in KBO.

10. Conclusions

Good quality and transparent single crystals of KBO crystal have been grown successfully in double distilled water by slow evaporation method. Single crystal X-ray diffraction analysis confirms the crystal system and lattice parameters. The functional groups present in the title compound were confirmed by FT-IR analysis. Optical transmission studies showed that KBO crystal was optically transparent. The dielectric constant and dielectric loss were measured as a function of frequency at 300 K. The microhardness studies reveal that the hardness of crystal is moderately good. The powder Kurtz method was used to confirm the second harmonic generation in the grown crystal. The crystal possesses a relatively large specific heat. All these properties show that the titled material may be a promising candidate for the fabrication of NLO devices.

Acknowledgements

The scientific supports extended by Sophisticated Analytical Instruments Facility, Indian Institute of Technology, Chennai and Indian Institute of Science (IISc) are gratefully acknowledged.

References

[1] R.W. Boyd, *Nonlinear Optics* (Academic Press, Inc., San Diego, 1992).
[2] B.E.A. Saleh, M.C. Teich, *Fundamentals of Photonics* (John Wiley & Sons, New York, 1991).
[3] M.H. Jiang, Q. Fang // *Adv. Mater.* **11** (1999) 1147.
[4] M.D. Aggarwal, J. Choi, W.S. Wang, K. Bhat, R.B. Lal, A.D. Shields, B.G. Penn, D.V. Frazier // *J. Cryst. Growth* **179** (1999) 2004.
[5] F. Zernike, J.E. Midwinter, *Applied Nonlinear Optics* (Wiley, New York, 1973).
[6] P.N. Prasad, D.J. Williams, *Introduction to Nonlinear Effects in Molecules and Polymers* (Wiley, New York, 1991).
[7] Dongfeng Xue, Siyuan Zhang // *Phys. B* **262** (1999) 78.

[8] Dongfeng Xue, Siyuan Zhang // *Chem. Phys. Lett.* **301** (1999) 449.
[9] Daqiu Yu, Dongfeng Xue, Henryk Ratajczak // *J. Mol. Struct.* **792** (2006) 280.
[10] S. Dhanuskodi, K. Vasantha // *Spectrochimica Acta A* **61** (2005) 1777.
[11] C. Justin Raj, S. Krishnan // *Crystal Growth and Design* **8(11)** (2008) 3956.
[12] V. Chithambaram, S. Jerome Das, R. Arivudai Nambi, S. Krishnan // *Optics & Laser Technology* **43** (2011) 1229.
[13] R. Shankar, C.M. Raghavan, M. Balaji, R. Mohan Kumar, R. Jayavel // *Crystal Growth Design* **7** (2007) 348.
[14] R.M. Silverstein, F.X. Webster, *Spectrometric Identification of Organic Compounds* (John Wiley & Sons, USA, 1997).
[15] B.C. Smith, *Quantitative Spectroscopy: Theory and Practice* (Elsevier, Amsterdam, 2002).
[16] M.M. Khandpekar, S.P. Pati // *Optics Communication* 283 (2010) 2700.
[17] K.V. Rao, A. Smakula // *J. Appl. Phys.* **36** (1965) 3953.
[18] C.P. Symth, *Dielectric behaviour and structure* (McGraw-Hill, New York, 1965).
[19] K.V. Rao, A. Smakula // *J. Appl. Phys.* **36** (1965) 2031.
[20] C. Balarew, R.J. Duhlew // *Solid State Chemistry* **55** (1984) 1.
[21] B.R. Lawn, E.R. Fuller // *J. Mater. Sci.* **9** (1975) 2016.
[22] Keyan Li, Xingtao Wang, Fangfang Zhang, Dongfeng Xue // *Phys. Rev. Lett.* **100** (2008) 235504.
[23] L.I. Keya, Xue Dongfeng // *Chin. Sci. Bull*. **54** (2009) 131.
[24] Keyan Li, Dongfeng Xue // *Phys. Scr.* **T139** (2010) 014073.
[25] D. Arirouli, R. Fomari, J. Kumar // *J. Mater. Sci. Lett*. **10** (1991) 559.
[26] J. Bent Charles, F.D. Gnanm // *J. Mater-Sci. Lett.* **10** (1991) 559.
[27] E. Chacko, J. Mary Linet, S. Mary Navis, Priya C. Vesta, B. Milton Boaz, S. Jerome Das // *Indian J. Pure Appl. Phys.* **44** (2006) 260.
[28] J. Gong // *J. Mater. Sci. Lett.* **19** (2000) 515.
[29] B.W. Mott, *Micro Indentation Hardness Testing* (Butterworths, London, 1966).
[30] K. Jagannathan, S. Kalainathan, T. Gnanasekaran // *Mater. Lett.* **61** (2007) 4485.
[31] S. Jerome Das, R. Gopinathann // *Cryst. Res. Technology* **21** (1992) 17.
[32] E.M. Onitsch // *Microskope* **95** (1950) 12.
[33] M. Hanneman // *Metall. Manch.* **23** (1941) 135.
[34] N. Pattanaboonmee, P. Ramasamy, R. Yimniruna, P. Manyuman // *Journal of Crystal Growth* **314** (2011) 196.
[35] S.K. Kurtz, T.T. Perry // *J. Appl. Phys.* **39** (1968) 3798.
[36] P.A. Franken, A.E. Hill, C.W. Peters, G. Weinreich // *Phys. Rev. Lett.* **7** (1961) 118.